HIGHLIGHTS FROM THE ATLAS EXPERIMENT*

Dominik Derendarz

on behalf of the ATLAS Collaboration

Institute of Nuclear Physics Polish Academy of Sciences
Radzikowskiego 152, 31-342 Kraków, Poland

Received 30 October 2022, accepted 7 November 2022, published online 14 December 2022

This report highlights some of the new results presented in 13 talks and 8 posters by the ATLAS Collaboration at the Quark Matter 2022 Conference. Particular emphasis is given to the most recent results regarding the production of jets, quarkonia, heavy-flavor quarks, collective effects, and photon-induced processes in ultra-peripheral collisions.

DOI:10.5506/APhysPolBSupp.16.1-A3

1. Introduction

Heavy-ion collisions provide a rich and complex laboratory for a wide physics program, focused on the study of quantum chromodynamics in a hot and dense matter [1]. In addition, in ultra-peripheral collision (UPC) events, electromagnetic fields surrounding accelerated nuclei give rise to many photon-induced processes such as light-by-light scattering or photonuclear interactions.

During the LHC Run 2 in 2015–2018, several runs dedicated to heavy-ion physics were performed, resulting in the main dataset corresponding to 2.2 nb^{-1} of Pb+Pb collisions at $\sqrt{s_{NN}} = 5.02$ TeV, complemented by reference pp collisions at the same energy. In addition, p+Pb collisions at $\sqrt{s_{NN}} = 5.02$ and 8.16 TeV, and a short pilot run of Xe+Xe collisions at $\sqrt{s_{NN}} = 5.44$ TeV were also carried out. The ATLAS experiment [2] at the LHC has undertaken an extensive program of measurements in all of those collision systems. In this report, the most recent ATLAS results on the production of jets, quarkonia, heavy-flavour quarks, and collective effects measured in Pb+Pb, p+Pb, and pp collisions will be presented. Results on electromagnetic processes studied in UPC will also be discussed as they are an integral part of the heavy-ion physics program with sensitivity to study nuclear PDFs, precision QED, and even new physics searches.

* Presented at the 29$^{\text{th}}$ International Conference on Ultrarelativistic Nucleus–Nucleus Collisions: Quark Matter 2022, Kraków, Poland, 4–10 April, 2022.

2. Bulk particle production

The presence of significant azimuthal anisotropy in nucleus–nucleus collisions is one of the most important arguments for the formation of a hot and dense quark–gluon plasma (QGP). Observation of the flow signal in small systems such as pp and p+Pb and the understanding of its origin is still an interesting open question, despite many studies performed so far. Recent ATLAS measurements explore details of azimuthal anisotropy in both small and large systems.

The interplay between the size and shape of the initial state was studied by measuring the strength of the correlation, ρ_n, between flow harmonics, v_n, and mean transverse momentum, $[p_{\mathrm{T}}]$ [3]. Recently, the measurement of ρ_2 was extended to the Xe+Xe system [4] and reveals the sensitivity of this observable to the nuclear deformation of the Xe nuclei. In figure 1 (left), the TRENTo model predictions for the ρ_2 ratio between Xe+Xe and Pb+Pb systems are presented for different assumptions on the Xe nuclear deformation. The measured ratio suggests that the Xe nucleus is a highly deformed triaxial ellipsoid that has neither a prolate nor an oblate shape.

To improve the understanding of the longitudinal structure of QGP, the system-size dependence of longitudinal decorrelations of v_n harmonics in the Xe+Xe system was investigated and compared to that measured in Pb+Pb [5]. It was found that current models tuned to describe the transverse dynamics characterized by v_n harmonics do not describe the longitudinal structure of the initial-state geometry.

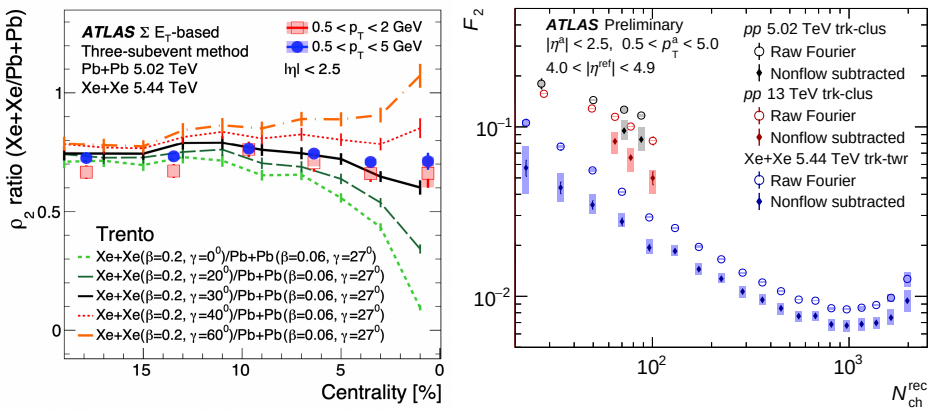

Fig. 1. Left: Comparison of ρ_2 ratios ($\rho_{2,\mathrm{Xe+Xe}}/\rho_{2,\mathrm{Pb+Pb}}$) with the TRENTo model for various quadrupole deformation parameter values in two p_{T} ranges as a function of centrality [4]. Right: The flow decorrelation F_2 parameter in pp and Xe+Xe collisions [6] as a function of a number of reconstructed charged particle tracks ($N_{\mathrm{ch}}^{\mathrm{rec}}$). For each system, raw and non-flow subtracted F_2 are shown.

Recently, the measurement of the longitudinal flow decorrelation was extended to an even smaller system, *pp* collisions [6]. Due to the larger influence of non-flow effects in small collision systems, dedicated template-based subtraction procedures were developed for this measurement. The strength of the decorrelation, F_2, [6] measured in *pp* and Xe+Xe collisions is shown in figure 1 (right). F_2 is a slope parameter of the ratio of flow vectors measured at different pseudorapidity intervals obtained via a simple linear regression. As a function of the number of reconstructed charged particle tracks, $N_{\mathrm{ch}}^{\mathrm{rec}}$, the decorrelations follow a similar pattern of large F_2 at low $N_{\mathrm{ch}}^{\mathrm{rec}}$ and decreasing with increasing multiplicity, however, it is substantially larger in *pp* collisions than in Xe+Xe collisions for the events with the same $N_{\mathrm{ch}}^{\mathrm{rec}}$. These results provide important information on the initial longitudinal dynamics in small collision systems.

3. Heavy flavour

Using the full statistics of data collected in 2015 and 2018, the production rates of the three Υ bottomonium states in Pb+Pb collisions have been compared with those in *pp* collisions to extract the nuclear modification factors as functions of event centrality and other kinematic variables [7]. In addition, the in-medium suppression of the Υ excited states relative to the ground state was studied. Theoretical computations incorporating deconfinement as a key ingredient in the suppression describe the Υ yields well.

Comprehensive and systematic studies of modification of heavy-flavour (HF) hadron production and flow in Pb+Pb collisions [8] probed via muons from semi-leptonic decays were complemented by the measurement of the azimuthal correlations of muon pairs from the HF decays [9]. As expected, significant suppression of the HF–muon pairs from peripheral-to-central collisions is observed. However, the widths of the muons' angular correlation do not show a significant modification with centrality.

To investigate the properties of the system in high-multiplicity *pp* collisions where flow signals are clearly established, the multiplicity and distributions of kinematic variables of charged particles produced in association with an Υ meson have been measured [10]. The measurement is performed separately for the first three $\Upsilon(nS)$ states in several intervals of Υ transverse momenta. At an Υ transverse momentum close to zero, the associated charged particle multiplicity is measured to be smaller by $12 \pm 1\%$ in collisions where an $\Upsilon(2S)$ is observed compared to the collisions with $\Upsilon(1S)$. For $\Upsilon(3S)$, this difference is $17 \pm 4\%$. This measurement quantifying the underlying event activity provides new data for models that describe the Υ meson production.

4. Jets

Using the heavy-ion data collected in 2015 and 2018, a comprehensive set of studies of the jet quenching phenomenon in the quark–gluon plasma has been performed.

The path-length dependence of jet quenching was studied by measuring the distribution of the dijet momentum balance, x_J, the ratio of the transverse momentum of the subleading jet to the transverse momentum of the leading jet, as a function of the p_{T} of the leading jet and collision centrality [11]. Even at the highest leading jet p_{T} measured, $398 < p_{\mathrm{T}} < 562$ GeV, significant modification from the shape in pp collisions is observed in Pb+Pb collisions. The absolutely normalized x_J distribution, *i.e.* normalized by the number of events scaled by the nuclear thickness function instead of per jet-pair normalization, shows that the observed difference with respect to pp collisions comes from the suppression of balanced dijet pairs and not as a result of an enhancement of imbalanced jets. An additional benefit of absolute normalization of x_J distributions is the possibility of constructing a nuclear modification factor, R_{AA}, for dijets as a function of the leading and subleading jet p_{T}. As shown in the left panel of figure 2, subleading jets are more suppressed than leading jets.

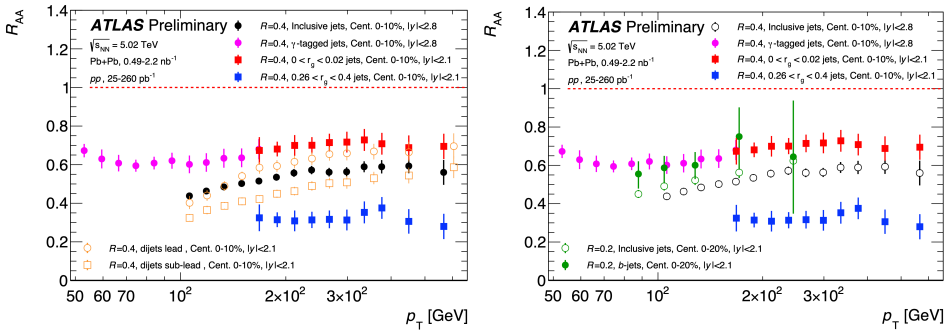

Fig. 2. (Colour on-line) Nuclear modification factor, R_{AA}, as a function of jet p_{T} of anti-k_{T} $R = 0.4$ gamma-tagged jets [12] (pink/grey filled circles) and inclusive jets [13] (black circles) at $|y| < 2.8$, soft-drop groomed jet [14] for narrow (red/grey squares) and wide (blue/black squares) r_g at $|y| < 2.1$ in 0–10% centrality interval. Left: R_{AA} of leading and subleading jets (orange/light grey empty squares and circles) from dijet pair [11] with $|y| < 2.1$ in centrality 0–10%. Right: Anti-k_{T} $R = 0.2$ b-jets [15] and inclusive jets at $|y| < 2.1$ in centrality 0–20% are shown in green/light grey filled and empty circles.

For the first time in ATLAS, the jet substructure modification and suppression have been measured in Pb+Pb collisions [14]. The jet nuclear modification factor has been observed to depend significantly on the jet r_g (an-

gular scale of the first hard splitting), with the production of jets with the largest measured r_g found to be twice as suppressed compared to those with the smallest r_g in central Pb+Pb collisions. The r_g and p_{T} dependence of the jet R_{AA} is qualitatively consistent with a picture of jet quenching arising from coherence and provides the most direct evidence in support of this approach.

ATLAS also presented two studies aimed to test the sensitivity of jet quenching to the type of initiating parton. The first measurement relies on the fact that jets produced in association with an isolated photon or electroweak boson are significantly more likely to be initiated by a quark compared to inclusive jets at the same p_{T}. The R_{AA} of jet produced opposite in azimuth to the high-p_{T} isolated photon is found to be significantly higher than that for inclusive jets indicating that parton energy loss is sensitive to the colour charge of the initiating parton [12]. In the second measurement, the production of b-jets in Pb+Pb and pp collisions has been studied [15]. The b-jets are identified statistically from a sample of jets containing muons, by the difference between muon transverse momenta relative to the jet+μ axis of the decays of the bottom-, charm-, and light-hadrons. Although limited in precision, the measurement of b-jet R_{AA} shows smaller suppression than that observed for inclusive jets. This suggests a dependence of mass and colour-charge effects on partonic energy loss in heavy-ion collisions.

Figure 2 illustrates a complex picture of jet quenching dependence on medium geometry, jet structure, and type of the parton interacting with the QGP.

The presence of significantly non-zero v_2 of high-p_{T} tracks [16], typically interpreted as a consequence of path-length-dependent energy loss in an elliptically shaped medium [17], rekindled the interest in the search of jet quenching effects in p+Pb collisions. The yield of charged hadrons correlated with reconstructed jets, $I_{p\mathrm{Pb}}$, was studied in p+Pb collisions [18]. A similar observable constructed from the yields of charged hadrons produced opposite in azimuth to Z boson in Pb+Pb collisions [19] shows significant modification consistent with the change of fragmentation of jets in the presence of QGP. In p+Pb and pp collisions, the $I_{p\mathrm{Pb}}$ was found to be consistent with unity. These data provide new, strong constraints which preclude almost any parton energy loss in central p+Pb collisions.

5. Photon-induced processes

Measurements of exclusive production of dilepton pairs, $\gamma\gamma \to l^+l^-$, in all lepton generations (e, μ, and τ) were performed by ATLAS using data from UPC collisions. Good statistics allow for a precise measurement of $\gamma\gamma \to e^+e^-$ [20] and $\gamma\gamma \to \mu^+\mu^-$ [21] cross sections that are in good agreement

with the QED predictions. Those measurements provide stringent tests of the current theoretical understanding of the photon fluxes generated by a nucleus and lay the foundation for the measurements that depend crucially on the understanding of the photon flux. The statistically limited $\gamma\gamma \to \tau^+\tau^-$ process has been observed with a significance exceeding 5 standard deviations and its signal strength was found in agreement with the Standard Model prediction [22]. The data are also used to constrain the anomalous magnetic moment of the τ-lepton, a_τ, with a sensitivity comparable to LEP results, as shown in figure 3.

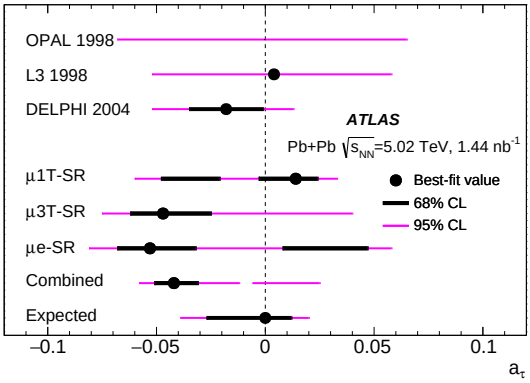

Fig. 3. Measurements of a_τ from fits to individual signal regions and from the combined fit [22]. Measurements from the OPAL, L3, and DELPHI at LEP are compared with the ATLAS result.

A finalized measurement of the dimuon photoproduction in non-ultra-peripheral Pb+Pb collisions confirms a previous observation of a centrality-dependent broadening of the acoplanarity distribution [23]. Recent theoretical calculations show that the broadening of acoplanarity could be a result of the impact-parameter dependence of photon fluxes and not necessarily due to the interaction of the dimuons with the magnetic field generated by the charge flow in the QGP.

The study of the production of jets in photo-nuclear collisions [24] provides an important step towards the goal of a precise estimate of nuclear PDFs. Photo-nuclear events were selected by requiring no breakup of one of the incident nuclei and using a rapidity gap requirement in the photon-going direction. The hard-scattering kinematics were reconstructed from the mass and rapidity of the jet system. This allows for a triple-differential cross-section measurement as a function of the nuclear and photon–parton momentum fractions, x_A and z_γ, and the total transverse momentum of the jet system, H_T. As an example, figure 4 shows result in the intermediate range of z_γ for the x_A distribution, reaching low x_A values where nuclear shadowing effects are expected to occur, for different H_T intervals.

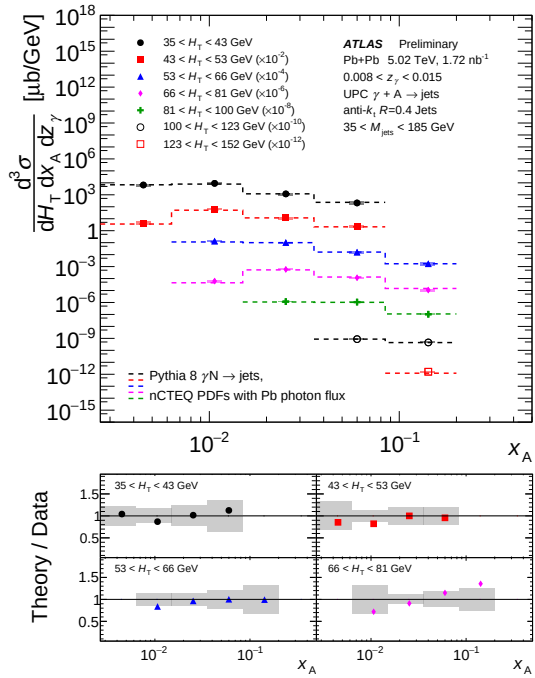

Fig. 4. Triple-differential cross sections for the jets production in photo-nuclear collisions as a function of x_{A} for different bins of H_{T} and photon energies in the range of $0.008 < z_{\gamma} < 0.015$ [24]. The bottom panels show the ratio between the theory prediction and data for several bins of H_{T}.

6. Summary

This report briefly highlights the latest results on the collectivity in *pp*, *p*+Pb, and nucleus–nucleus collisions, results on penetrating probes of QGP in Pb+Pb collisions, and results on the photon-induced processes in ultra-peripheral collisions. These new measurements by ATLAS should help to answer many open questions in the field and set the stage for an exciting program of heavy-ion physics in the LHC Run 3 and Run 4 [25].

REFERENCES

[1] W. Busza, K. Rajagopal, W. van der Schee, *Annu. Rev. Nucl. Part. Sci.* **68**, 339 (2018), arXiv:1802.04801 [hep-ph].

[2] ATLAS Collaboration (G. Aad *et al.*), *J. Instrum.* **3**, S08003 (2008).

[3] ATLAS Collaboration (G. Aad *et al.*), *Eur. Phys. J. C* **79**, 985 (2019), arXiv:1907.05176 [nucl-ex].

[4] ATLAS Collaboration, arXiv:2205.00039 [nucl-ex], accepted by *Phys. Rev. C*.

[5] ATLAS Collaboration (G. Aad *et al.*), *Phys. Rev. Lett.* **126**, 122301 (2021), arXiv:2001.04201 [nucl-ex].

[6] ATLAS Collaboration, ATLAS-CONF-2022-020.

[7] ATLAS Collaboration, arXiv:2205.03042 [nucl-ex], accepted by *Phys. Rev. C*.

[8] ATLAS Collaboration, *Phys. Lett. B* **829**, 137077 (2022), arXiv:2109.00411 [nucl-ex].

[9] ATLAS Collaboration, ATLAS-CONF-2022-022.

[10] ATLAS Collaboration, ATLAS-CONF-2022-023.

[11] ATLAS Collaboration, arXiv:2205.00682 [nucl-ex], accepted by *Phys. Rev. C*.

[12] ATLAS Collaboration, ATLAS-CONF-2022-019.

[13] ATLAS Collaboration, *Phys. Lett. B* **790**, 108 (2019), arXiv:1805.05635 [hep-ex].

[14] ATLAS Collaboration, ATLAS-CONF-2022-026.

[15] ATLAS Collaboration, arXiv:2204.13530 [nucl-ex], accepted by *Eur. Phys. J. C*.

[16] ATLAS Collaboration (G. Aad *et al.*), *Eur. Phys. J. C* **80**, 73 (2020), arXiv:1910.13978 [nucl-ex].

[17] ATLAS Collaboration (G. Aad *et al.*), *Phys. Rev. C* **105**, 064903 (2022), arXiv:2111.06606 [nucl-ex].

[18] ATLAS Collaboration, arXiv:2206.01138 [nucl-ex], submitted to *Phys. Rev. Lett.*

[19] ATLAS Collaboration (G. Aad *et al.*), *Phys. Rev. Lett.* **126**, 072301 (2021), arXiv:2008.09811 [nucl-ex].

[20] ATLAS Collaboration, arXiv:2207.12781 [nucl-ex], submitted to *J. High Energy Phys.*

[21] ATLAS Collaboration (G. Aad *et al.*), *Phys. Rev. C* **104**, 024906 (2021), arXiv:2011.12211 [nucl-ex].

[22] ATLAS Collaboration, arXiv:2204.13478 [hep-ex], accepted by *Phys. Rev. Lett.*

[23] ATLAS Collaboration, arXiv:2206.12594 [nucl-ex], submitted to *Phys. Rev. C*.

[24] ATLAS Collaboration, ATLAS-CONF-2022-021.

[25] Z. Citron *et al.*, arXiv:1812.06772 [hep-ph].